Eur. Phys. J. C (2019) 79:887
https://doi.org/10.1140/epjc/s10052-019-7419-7

THE EUROPEAN PHYSICAL JOURNAL C

Regular Article - Theoretical Physics

Molecular states from $\Sigma_c^{(*)}\bar{D}^{(*)} - \Lambda_c\bar{D}^{(*)}$ interaction

Jun He[1,a], **Dian-Yong Chen**[2]

[1] Department of Physics and Institute of Theoretical Physics, Nanjing Normal University, Nanjing 210097, China
[2] School of Physics, Southeast University, Nanjing 210094, China

Received: 15 September 2019 / Accepted: 19 October 2019 / Published online: 4 November 2019

Abstract In this work, we systemically investigate the molecular states from the $\Sigma_c^{(*)}\bar{D}^{(*)}-\Lambda_c\bar{D}^{(*)}$ interaction with the help of the Lagrangians with heavy quark and chiral symmetries in a quasipotential Bethe–Salpeter equation (qBSE) approach. The molecular states are produced from isodoublet (I=1/2) $\Sigma_c\bar{D}$ interaction with spin parity $J^P = 1/2^-$ and $\Sigma_c\bar{D}^*$ interaction with $1/2^-$ and $3/2^-$. Their masses and widths are consistent with the $P_c(4312)$, $P_c(4440)$ and $P_c(4457)$ observed at LHCb. The states, $\Sigma_c^*\bar{D}^*(1/2^-)$, $\Sigma_c^*\bar{D}^*(3/2^-)$ and $\Sigma_c^*\bar{D}(3/2^-)$, are also produced with the same parameters. The isodoublet $\Sigma_c^*\bar{D}^*$ interaction with $5/2^-$, as well as the isoquartet (I=3/2) $\Sigma_c\bar{D}^*$ interactions with $1/2^-$ and $3/2^-$, $\Sigma_c^*\bar{D}^*$ interaction with $3/2^-$ and $5/2^-$, are also attractive while very large cutoff is required to produce a molecular state. We also investigate the origin of the widths of these molecular states in the same qBSE frame. The $\Lambda\bar{D}^*$ channel is dominant in the decays of the states, $\Sigma_c\bar{D}^*(1/2^-)$, $\Sigma_c\bar{D}^*(3/2^-)$, $\Sigma_c^*\bar{D}(3/2^-)$, and $\Sigma_c\bar{D}(1/2^-)$. The $\Sigma_c^*\bar{D}^*(1/2^-)$ state has large coupling to $\Sigma_c\bar{D}$ channel while the $\Sigma_c\bar{D}^*$, $\Sigma_c^*\bar{D}$ and $\Lambda_c\bar{D}^*$ channels provide similar contributions to the width of the $\Sigma_c^*\bar{D}^*(3/2^-)$ state. These results will be helpful to understand the current LHCb experimental results, and the three predicted states and the decay pattern of these hidden-charmed molecular pentaquarks can be checked in future experiments.

1 Introduction

The study of exotic hadrons is an important topic in understanding how quarks combine to a hadron. One type of the exotic hadrons is the molecular state, which is a shallow bound state of two and more hadrons. Though it is not so fancy as a compact multiquark, it seems easier to be produced because its constituent hadrons are realistic. In the side of experiment, many XYZ particles were observed near the threshold of charmed-anticharmed or bottom-antibottom mesons. For example, the $X(3872)/Z_c(3900)$, $Z_c(4020)$, $Z_b(10610)$ and $Z_b(10650)$ are very close to the $D\bar{D}^*$, $D^*\bar{D}^*$, $B\bar{B}^*$ and $B^*\bar{B}^*$ thresholds, respectively. It suggests that such particles are from the interactions of the corresponding hadrons. It also makes the molecular state picture become a popular interpretation of the XYZ particles.

Recently, the LHCb Collaboration updated their observation of pentaquark candidates [1]. The upper one, $P_c(4450)$, resolves into two resonances, $P_c(4440)$ and $P_c(4457)$, and a new pentaquark, $P_c(4312)$, was observed near the $\Sigma_c\bar{D}$ threshold. The $P_c(4380)$ reported in the previous observation [2] is suspended to wait construction of new amplitude model. The four pentaquarks, $P_c(4457)$, $P_c(4440)$, $P_c(4380)$, and $P_c(4312)$, construct a good pattern for all S-wave molecular states from $\Sigma_c\bar{D}^*$, $\Sigma_c^*\bar{D}$, and $\Sigma_c\bar{D}$ interactions, which has been predicted partly in the literature [3–6]. After the LHCb results released, many theoretical interpretations in the molecular state picture were proposed [7–20].

To further confirm the molecular state interpretation of the P_c states, it is very helpful to make a prediction of more states with the relevant interactions. The four P_c states observed at LHCb are all from the $\Sigma_c^{(*)}\bar{D}^{(*)}$ interaction. If we only consider the S-wave states, there should be seven possible molecular states. The states from the $\Sigma_c\bar{D}$, $\Sigma_c^*\bar{D}$, and $\Sigma_c\bar{D}^*$ interactions have been filled by the experimental observed $P_c(4312)$, $P_c(4380)$, $P_c(4440)$, and $P_c(4457)$. It is interesting to find out if there exist three S-wave $\Sigma^*\bar{D}^*$ molecular states. In Refs. [21–23], such states has been studied in a parameterized model, and the authors suggested the existence of three $\Sigma^*\bar{D}^*$ states with the observed P_c states as input.

Theoretically, a state usually exhibits different decay behaviors in different theoretical pictures. The decay pattern of the pentaquarks is another way to check their internal structure. In the literature, the decays of the P_c states have been studied by many authors [24–26]. In Ref. [25], it was suggested that the $\Lambda_c\bar{D}^*$ channel is very important in the

[a] e-mail: junhe@njnu.edu.cn

decays of the P_c states. The mass and the decay pattern of a molecular state is often studied separately in the literature. If the P_c states are molecular states from the $\Sigma_c^{(*)}\bar{D}^{(*)}$ interaction, the decays to these channels can be obtained as a coproduct after the coupled-channel effect is included. A bound state will acquire a width, and exhibits itself as a pole in the complex plane after adding another interaction channel below the production channel to make a coupled-channel calculation. Hence, it is interesting to study the production of the molecular states produced from the interaction and their decay behaviors in the same theoretical frame.

In our previous work [27], we studied the $\Sigma_c^{(*)}\bar{D}^{(*)}$ interaction and focused on the molecular states which can be related to the three pentaquarks observed at LHCb. A calculation in a quasipotential Bethe–Salpeter equation (qBSE) approach suggests that the $P_c(4457)$, $P_c(4440)$ and $P_c(4312)$ can be explained as two $\Sigma_c\bar{D}^*$ molecular states with $3/2^-$ and $1/2^-$ and a $\Sigma_c\bar{D}$ molecular state with $1/2^-$. An enhancement was also found near the $\Sigma_c^*\bar{D}$ threshold with $3/2^-$. It is naturally to extend the calculation to study all possible S-wave isodoublet ($I = 1/2$) molecular states from the $\Sigma_c^{(*)}\bar{D}^{(*)}$ interaction and their isoquartet ($I = 3/2$) partners. The previous calculation suggests that the coupled-channel effect between different channels is small for the molecular states related to the $P_c(4312)$, $P_c(440)$, and $P_c(4457)$, which leads to very small widths if only $\Sigma_c^{(*)}\bar{D}^{(*)}$ interaction considered. The widths of those states are possible from the coupling to $\Lambda_c\bar{D}^*$ channel as suggested in Ref. [25]. Hence, in the current work, we will make a systemically calculation of the $\Sigma_c^{(*)}\bar{D}^{(*)} - \Lambda_c\bar{D}^{(*)}$ interaction in the qBSE approach to find out all possible S-wave molecular states and to study the couplings of these channels in the same frame.

This work is organized as follows. After introduction, the detail of the dynamical study of coupled-channel $\Sigma_c^{(*)}\bar{D}^{(*)} - \Lambda_c\bar{D}^{(*)}$ interactions will be presented, which includes relevant effective Lagrangians, reduction of potential kernel and a brief introduction of the qBSE. Then, the results of shingle-channel calculation are given in Sect. 3 to present the possible bound states produced form the $\Sigma_c^{(*)}\bar{D}^{(*)} - \Lambda_c\bar{D}^{(*)}$ interaction. The coupled-channel results are presented in Sect. 4. The bound states obtained in Sect. 3 become poles in complex plane, which will be compared with the experimental results. The poles of the molecular states from full coupled-channel and two-channel calculations will be presented also, which can be related to their decay widths. Finally, summary and discussion will be given in the last section.

2 Theoretical frame

To study the bound states from the $\Sigma_c^{(*)}\bar{D}^{(*)} - \Lambda_c\bar{D}^{(*)}$ interaction and the couplings between different channels, we need to construct the coupled-channel potential kernel. In the current work, we adopt the one-boson-exchange model to describe the interaction between the charmed baryon and anticharmed meson. The exchanges by peseudoscalar $\mathbb{P}$, vector $\mathbb{V}$ and σ mesons will be considered. Hence, the effective Lagrangians depicting the couplings of light mesons and anticharmed mesons or charmed baryons are required and will be presented in the below.

2.1 Relevant Lagrangians

First, we consider the couplings of light mesons to heavy-light anticharmed mesons $\tilde{\mathcal{P}} = (\bar{D}^0, D^-, D_s^-)$. In terms of heavy quark limit and chiral symmetry, the Lagrangians have been constructed in the literature as [28–31],

$$\begin{aligned}
\mathcal{L}_{HH\mathbb{P}} &= ig_1\langle \bar{H}_a^{\bar{Q}}\gamma_\mu A^\mu_{ba}\gamma_5 H_b^{\bar{Q}}\rangle,\\
\mathcal{L}_{HH\mathbb{V}} &= -i\beta\langle \bar{H}_a^{\bar{Q}} v_\mu(\mathcal{V}^\mu_{ab} - V^\mu_{ab})H_b^{\bar{Q}}\rangle\\
&\quad + i\lambda\langle \bar{H}_b^{\bar{Q}}\sigma_{\mu\nu}F^{\mu\nu}(\rho)\bar{H}_a^{\bar{Q}}\rangle,\\
\mathcal{L}_{HH\sigma} &= g_s\langle \bar{H}_a^{\bar{Q}}\sigma\bar{H}_a^{\bar{Q}}\rangle,
\end{aligned} \tag{1}$$

where the axial current is $A^\mu = \frac{1}{2}(\xi^\dagger\partial_\mu\xi - \xi\partial_\mu\xi^\dagger) = \frac{i}{f_\pi}\partial_\mu\mathbb{P} + \cdots$ with $\xi = \exp(i\mathbb{P}/f_\pi)$ and $f_\pi = 132$ MeV. $\mathcal{V}_\mu = \frac{i}{2}[\xi^\dagger(\partial_\mu\xi) + (\partial^\mu\xi)\xi^\dagger] = 0$. $V^\mu_{ba} = ig_{\mathbb{V}}\mathbb{V}^\mu_{ba}/\sqrt{2}$, and $F_{\mu\nu}(\rho) = \partial_\mu V_\nu - \partial_\nu V_\mu + [\rho_\mu,\ \rho_\nu]$. The $\mathbb{P}$ and $\mathbb{V}$ are the pseudoscalar and vector matrices as

$$\mathbb{P} = \begin{pmatrix} \frac{1}{\sqrt{2}}\pi^0 + \frac{\eta}{\sqrt{6}} & \pi^+ & K^+ \\ \pi^- & -\frac{1}{\sqrt{2}}\pi^0 + \frac{\eta}{\sqrt{6}} & K^0 \\ K^- & \bar{K}^0 & -\frac{2\eta}{\sqrt{6}} \end{pmatrix},$$

$$\mathbb{V} = \begin{pmatrix} \frac{\rho^0}{\sqrt{2}} + \frac{\omega}{\sqrt{2}} & \rho^+ & K^{*+} \\ \rho^- & -\frac{\rho^0}{\sqrt{2}} + \frac{\omega}{\sqrt{2}} & K^{*0} \\ K^{*-} & \bar{K}^{*0} & \phi \end{pmatrix}. \tag{2}$$

The $H_a^{\bar{Q}} = [\tilde{\mathcal{P}}_a^{*\mu}\gamma_\mu - \tilde{\mathcal{P}}_a\gamma_5]\frac{1-\not{v}}{2}$ and $\bar{H} = \gamma_0 H^\dagger\gamma_0$ with $v = (1, \mathbf{0})$. The $\tilde{\mathcal{P}}$ and $\tilde{\mathcal{P}}^*$ satisfy the normalization relations $\langle 0|\tilde{\mathcal{P}}|\bar{Q}q(0^-)\rangle = \sqrt{M_{\mathcal{P}}}$ and $\langle 0|\tilde{\mathcal{P}}^*_\mu|\bar{Q}q(1^-)\rangle = \epsilon_\mu\sqrt{M_{\mathcal{P}^*}}$.

The Lagrangians can be further expanded as follows,

$$\begin{aligned}
\mathcal{L}_{\tilde{\mathcal{P}}^*\tilde{\mathcal{P}}\mathbb{P}} &= i\frac{2g\sqrt{m_{\tilde{\mathcal{P}}}m_{\tilde{\mathcal{P}}^*}}}{f_\pi}(-\tilde{\mathcal{P}}^{*\dagger}_{a\lambda}\tilde{\mathcal{P}}_b + \tilde{\mathcal{P}}^\dagger_a\tilde{\mathcal{P}}^*_{b\lambda})\partial^\lambda\mathbb{P}_{ab},\\
\mathcal{L}_{\tilde{\mathcal{P}}^*\tilde{\mathcal{P}}^*\mathbb{P}} &= -\frac{g}{f_\pi}\epsilon_{\alpha\mu\nu\lambda}\tilde{\mathcal{P}}^{*\mu\dagger}_a\overleftrightarrow{\partial}^\alpha\tilde{\mathcal{P}}^{*\lambda}_b\partial^\nu\mathbb{P}_{ba},\\
\mathcal{L}_{\tilde{\mathcal{P}}^*\tilde{\mathcal{P}}\mathbb{V}} &= \sqrt{2}\lambda g_V\varepsilon_{\lambda\alpha\beta\mu}(-\tilde{\mathcal{P}}^{*\mu\dagger}_a\overleftrightarrow{\partial}^\lambda\tilde{\mathcal{P}}_b\\
&\quad + \tilde{\mathcal{P}}^\dagger_a\overleftrightarrow{\partial}^\lambda\tilde{\mathcal{P}}^{*\mu}_b)(\partial^\alpha\mathbb{V}^\beta)_{ab},\\
\mathcal{L}_{\tilde{\mathcal{P}}\tilde{\mathcal{P}}\mathbb{V}} &= -i\frac{\beta g_V}{\sqrt{2}}\tilde{\mathcal{P}}^\dagger_a\overleftrightarrow{\partial}_\mu\tilde{\mathcal{P}}_b\mathbb{V}^\mu_{ab},\\
\mathcal{L}_{\tilde{\mathcal{P}}^*\tilde{\mathcal{P}}^*\mathbb{V}} &= -i\frac{\beta g_V}{\sqrt{2}}\tilde{\mathcal{P}}^{*\dagger}_a\overleftrightarrow{\partial}_\mu\tilde{\mathcal{P}}^*_b\mathbb{V}^\mu_{ab}\\
&\quad - i2\sqrt{2}\lambda g_V m_{\tilde{\mathcal{P}}^*}\tilde{\mathcal{P}}^{*\mu\dagger}_a\tilde{\mathcal{P}}^{*\nu}_b(\partial_\mu\mathbb{V}_\nu - \partial_\nu\mathbb{V}_\mu)_{ab},
\end{aligned}$$

$$\mathcal{L}_{\tilde{\mathcal{P}}\tilde{\mathcal{P}}\sigma} = -2g_s m_{\tilde{\mathcal{P}}} \tilde{\mathcal{P}}_a^\dagger \tilde{\mathcal{P}}_a \sigma,$$
$$\mathcal{L}_{\tilde{\mathcal{P}}^*\tilde{\mathcal{P}}^*\sigma} = 2g_s m_{\tilde{\mathcal{P}}^*} \tilde{\mathcal{P}}_a^{*\dagger} \tilde{\mathcal{P}}_a^* \sigma, \tag{3}$$

where the v is replaced by $i\overleftrightarrow{\partial}/\sqrt{m_i m_f}$ with the $m_{i,f}$ is for the initial or final $\bar{D}^{(*)}$ meson.

The Lagrangians for the couplings between the charmed baryon and light mesons can also be constructed in the heavy quark limit and under chiral symmetry as,

$$\begin{aligned}\mathcal{L}_S = &-\frac{3}{2} g_1(v_\kappa)\epsilon^{\mu\nu\lambda\kappa}\mathrm{tr}[\bar{S}_\mu A_\nu S_\lambda] \\ &+ i\beta_S \mathrm{tr}[\bar{S}_\mu v_\alpha(\mathcal{V}^\alpha - V^\alpha)S^\mu] \\ &+ \lambda_S \mathrm{tr}[\bar{S}_\mu F^{\mu\nu} S_\nu] + \ell_S \mathrm{tr}[\bar{S}_\mu \sigma S^\mu],\end{aligned} \tag{4}$$

$$\mathcal{L}_{B_{\bar{3}}} = i\beta_B \mathrm{tr}[\bar{B}_{\bar{3}} v_\mu(\mathcal{V}^\mu - V^\mu)B_{\bar{3}}] + \ell_B \mathrm{tr}[\bar{B}_{\bar{3}}\sigma B_{\bar{3}}], \tag{5}$$

$$\mathcal{L}_{int} = ig_4 \mathrm{tr}[\bar{S}^\mu A_\mu B_{\bar{3}}] + i\lambda_I \epsilon^{\mu\nu\lambda\kappa} v_\mu \mathrm{tr}[\bar{S}_\nu F_{\lambda\kappa} B_{\bar{3}}] + h.c., \tag{6}$$

where S_{ab}^μ is composed of Dirac spinor operators,

$$\begin{aligned}S_\mu^{ab} &= -\sqrt{\frac{1}{3}}(\gamma_\mu + v_\mu)\gamma^5 B^{ab} + B_\mu^{*ab} \equiv B_{0\mu}^{ab} + B_{1\mu}^{ab}, \\ \bar{S}_\mu^{ab} &= \sqrt{\frac{1}{3}}\bar{B}^{ab}\gamma^5(\gamma_\mu + v_\mu) + \bar{B}_\mu^{*ab} \equiv \bar{B}_{0\mu}^{ab} + \bar{B}_{1\mu}^{ab},\end{aligned} \tag{7}$$

and the the charmed baryon matrices are defined as

$$B_{\bar{3}} = \begin{pmatrix} 0 & \Lambda_c^+ & \Xi_c^+ \\ -\Lambda_c^+ & 0 & \Xi_c^0 \\ -\Xi_c^+ & -\Xi_c^0 & 0 \end{pmatrix},$$
$$B = \begin{pmatrix} \Sigma_c^{++} & \frac{1}{\sqrt{2}}\Sigma_c^+ & \frac{1}{\sqrt{2}}\Xi_c'^+ \\ \frac{1}{\sqrt{2}}\Sigma_c^+ & \Sigma_c^0 & \frac{1}{\sqrt{2}}\Xi_c'^0 \\ \frac{1}{\sqrt{2}}\Xi_c'^+ & \frac{1}{\sqrt{2}}\Xi_c'^0 & \Omega_c^0 \end{pmatrix}. \tag{8}$$

The explicit forms of the Lagrangians can be written as,

$$\begin{aligned}\mathcal{L}_{BB\mathbb{P}} &= i\frac{3g_1}{2f_\pi\sqrt{m_{\bar{B}}m_B}}\epsilon^{\mu\nu\lambda\kappa}\partial^\nu\mathbb{P}\sum_{i=0,1}\bar{B}_{i\mu}\overleftrightarrow{\partial}_\kappa B_{j\lambda}, \\ \mathcal{L}_{BB\mathbb{V}} &= -\frac{\beta_S g_V}{\sqrt{2m_{\bar{B}}m_B}}\mathbb{V}^\nu\sum_{i=0,1}\bar{B}_i^\mu\overleftrightarrow{\partial}_\nu B_{j\mu} \\ &\quad -\frac{\lambda_S g_V}{\sqrt{2}}(\partial_\mu\mathbb{V}_\nu - \partial_\nu\mathbb{V}_\mu)\sum_{i=0,1}\bar{B}_i^\mu B_j^\nu, \\ \mathcal{L}_{BB\sigma} &= \ell_S\sigma\sum_{i=0,1}\bar{B}_i^\mu B_{j\mu}, \\ \mathcal{L}_{B_{\bar{3}}B_{\bar{3}}\mathbb{V}} &= -\frac{g_V\beta_B}{\sqrt{2m_{\bar{B}_{\bar{3}}}m_{B_{\bar{3}}}}}\mathbb{V}^\mu\bar{B}_{\bar{3}}\overleftrightarrow{\partial}_\mu B_{\bar{3}}, \\ \mathcal{L}_{B_{\bar{3}}B_{\bar{3}}\sigma} &= i\ell_B\sigma\bar{B}_{\bar{3}}B_{\bar{3}}, \\ \mathcal{L}_{BB_{\bar{3}}\mathbb{P}} &= -i\frac{g_4}{f_\pi}\sum_i\bar{B}_i^\mu\partial_\mu\mathbb{P}B_{\bar{3}} + \mathrm{H.c.}, \\ \mathcal{L}_{BB_{\bar{3}}\mathbb{V}} &= \sqrt{\frac{2}{m_{\bar{B}}m_{B_{\bar{3}}}}}g_{\mathbb{V}}\lambda_I\epsilon^{\mu\nu\lambda\kappa}\partial_\lambda\mathbb{V}_\kappa\sum_i\bar{B}_{i\nu}\overleftrightarrow{\partial}_\mu B_{\bar{3}} + \mathrm{H.c.}.\end{aligned} \tag{9}$$

The coupling constants involve in the above Lagrangians should be determined to constrain the Lagrangians. In Table 1, we list the values of these coupling constants used in the calculation, which are cited from the literature [14,33–35].

In the calculation, the masses of particles are chosen as suggested values in the review of particle physics (PDG) [32]. The mass difference from the charge is neglected, and average mass is adopted. For example, the mass of the $\bar{D}$ meson is chosen as $(m_{\bar{D}^0} + m_{D^-})/2$. The effect of such treatment is negligible on the result and conclusion of this work. For the broad $\sigma/f_0(500)$ meson, only a range of the pole, $(400-550) - i(200-350)$, is provided in PDG. Here, we adopt a mass of 500 MeV. The different choices of the mass of σ meson from 400 to 550 MeV will effect the result a little, and can be smeared by a small variation of the cutoff.

2.2 Potential of $\Sigma_c^{(*)}\bar{D}^{(*)} - \Lambda_c\bar{D}^{(*)}$ interaction

The potential of the $\Sigma_c^{(*)}\bar{D}^{(*)} - \Lambda_c\bar{D}^{(*)}$ interaction can be constructed with the help of the vertices for the heavy meson/baryon and the exchanged light meson, which can be easily obtained from the above Lagrangians. Besides the vertices, the propagators of the exchanged light mesons are also needed, which read,

$$\begin{aligned}P_{\mathbb{P}}(q^2) &= \frac{i}{q^2 - m_{\mathbb{P}}^2}\,f_i(q^2), \\ P_{\mathbb{V}}^{\mu\nu}(q^2) &= i\frac{-g^{\mu\nu} + q^\mu q^\nu/m_{\mathbb{V}}^2}{q^2 - m_{\mathbb{V}}^2}\,f_i(q^2), \\ P_\sigma(q^2) &= \frac{i}{q^2 - m_\sigma^2}\,f_i(q^2),\end{aligned} \tag{10}$$

where the form factor $f_i(q^2)$ is adopted to compensate the off-shell effect of exchanged meson. In this work, we introduce four types of from factors to check the effect of the form factor on the results, which are in forms of

$$f_1(q^2) = \frac{\Lambda_e^2 - m_e^2}{\Lambda_e^2 - q^2}, \tag{11}$$

$$f_2(q^2) = \frac{\Lambda_e^4}{(m_e^2 - q^2)^2 + \Lambda^4}, \tag{12}$$

$$f_3(q^2) = e^{-(m_e^2 - q^2)^2/\Lambda_e^2}, \tag{13}$$

$$f_4(q^2) = \frac{\Lambda_e^4 + (q_t^2 - m_e^2)^2/4}{[q^2 - (q_t^2 + m_e^2)/2]^2 + \Lambda_e^4}, \tag{14}$$

where m_e and q are the mass and momentum of the exchanged light meson. The q_t^2 denotes the value of q^2 at the kinematical threshold. The cutoff is rewritten as a form of $\Lambda_e = m + \alpha_e$ 0.22 GeV. In the calculation we also consider the propagators without a form factor, we remark it as $f_0(q^2) = 1$.

Table 1 The parameters and coupling constants adopted in our calculation. The λ and $\lambda_{S,I}$ are in the unit of GeV^{-1}. Others are in the unit of 1

β	g	g_V	λ	g_s			
0.9	0.59	5.9	0.56	0.76			
β_S	ℓ_S	g_1	λ_S	β_B	ℓ_B	g_4	λ_I
−1.74	6.2	−0.94	−3.31	$-\beta_S/2$	$-\ell_S/2$	$g_1/\frac{2\sqrt{2}}{3}$	$-\lambda_S/\sqrt{8}$

Table 2 The flavor factors for certain meson exchanges of certain interaction. The values in bracket are for the case of $I = 3/2$ if the values are different from these of $I = 1/2$

	π	η	ρ	ω	σ
$\bar{D}^{(*)}\Sigma^{(*)}_c \to \bar{D}^{(*)}\Sigma^{(*)}_c$	$-1[\frac{1}{2}]$	$\frac{1}{6}[\frac{1}{6}]$	$-1[\frac{1}{2}]$	$\frac{1}{2}[\frac{1}{2}]$	1
$\bar{D}^{(*)}\Lambda_c \to \bar{D}^{(*)}\Lambda_c$	0	0	0	1	2
$\bar{D}^{(*)}\Lambda_c \to \bar{D}^{(*)}\Sigma^{(*)}_c$	$\frac{\sqrt{6}}{2}$	0	$\frac{\sqrt{6}}{2}$	0	0

Because six channels are considered in the current work, it is tedious and fallible to give the explicit of 36 potential elements for the potential of the coupled-channel interaction and input them into the code. Instead, in this work, we input the vertices Γ and the above propagators P into the code directly and the potential can be obtained as

$$\mathcal{V}_{\mathbb{P},\sigma} = f_I \Gamma_1 \Gamma_2 P_{\mathbb{P},\sigma}(q^2), \quad \mathcal{V}_{\mathbb{V}} = f_I \Gamma_{1\mu} \Gamma_{2\nu} P^{\mu\nu}_{\mathbb{V}}(q^2). \quad (15)$$

Hence, the explicit forms of the potentials are not given here. The f_I is the flavor factor for certain meson exchange of certain interaction. It can be derived with the Lagrangians in Eqs. (3) and (9) and the matrices in Eqs. (2) and (8). The explicit values are listed in Table 2.

2.3 The qBSE approach

The scattering amplitude can be calculated with the help of the potential of the interaction obtained in the above. The Bethe–Salpeter equation is widely used to treat two-body scattering. With a quasi potential approximation, the 4-dimensional Bethe–Salpeter equation can be reduced to a 3-dimensional equation and the unitary is kept. As our previous works [11,36–40], a spectator approximation, which was explained explicitly in the appendices of Ref. [37], will be adopted in this work to search the possible bound states. A bound state from the interaction corresponds to a pole of the scattering amplitude $\mathcal{M}$.

After partial-wave decomposition, the 3-dimensional Bethe-Saltpeter equation after spectator quasipotential approximation can be reduced further to a 1-dimensional equation with fixed spin-parity J^P as [37],

$$i\mathcal{M}^{J^P}_{\lambda'\lambda}(\mathrm{p}', \mathrm{p}) = i\mathcal{V}^{J^P}_{\lambda',\lambda}(\mathrm{p}', \mathrm{p}) + \sum_{\lambda''} \int \frac{\mathrm{p}''^2 d\mathrm{p}''}{(2\pi)^3} \cdot i\mathcal{V}^{J^P}_{\lambda'\lambda''}(\mathrm{p}', \mathrm{p}'') G_0(\mathrm{p}'') i\mathcal{M}^{J^P}_{\lambda''\lambda}(\mathrm{p}'', \mathrm{p}), \quad (16)$$

where the sum extends only over nonnegative helicity λ''. Here, the reduced propagator with the spectator approximation can be written down in the center-of-mass frame with $P = (W, \mathbf{0})$ as

$$G_0 = \frac{\delta^+(p''^2_h - m^2_h)}{p''^2_l - m^2_l} = \frac{\delta^+(p''^0_h - E_h(\mathrm{p}''))}{2E_h(\mathrm{p}'')[(W - E_h(\mathrm{p}''))^2 - E^2_l(\mathrm{p}'')]}. \quad (17)$$

Here, as required by the spectator approximation, the heavier particle (remarked with h) is on shell, which satisfies $p''^0_h = E_h(\mathrm{p}'') = \sqrt{m^2_h + \mathrm{p}''^2}$. The p''^0_l for the lighter particle (remarked as l) is then $W - E_h(\mathrm{p}'')$. Here and hereafter, a definition $\mathrm{p} = |\boldsymbol{p}|$ will be adopted.

The partial wave potential is defined with the potential of the interaction obtained in the above as

$$\mathcal{V}^{J^P}_{\lambda'\lambda}(\mathrm{p}', \mathrm{p}) = 2\pi \int d\cos\theta \left[d^J_{\lambda\lambda'}(\theta) \mathcal{V}_{\lambda'\lambda}(\boldsymbol{p}', \boldsymbol{p}) + \eta d^J_{-\lambda\lambda'}(\theta) \mathcal{V}_{\lambda'-\lambda}(\boldsymbol{p}', \boldsymbol{p}) \right], \quad (18)$$

where $\eta = P P_1 P_2 (-1)^{J-J_1-J_2}$ with P and J being parity and spin for system, $\bar{D}^{(*)}$ meson or $\Sigma^{(*)}_c$ baryon. The initial and final relative momenta are chosen as $\boldsymbol{p} = (0, 0, \mathrm{p})$ and $\boldsymbol{p}' = (\mathrm{p}' \sin\theta, 0, \mathrm{p}' \cos\theta)$. The $d^J_{\lambda\lambda'}(\theta)$ is the Wigner d-matrix.

One may note that we make the partial wave decomposition on the spin parity J^P, and the explicit orbital angular momentum L is not involved here. It is consistent with relativistic treatment adopted in the qBSE approach because the L is not a good quantum number in a relativistic theoretical frame. With such treatment, the contributions form all partial waves based on orbital angular momentum L related to a certain J^P considered have been included already. It is an advantage of our method because the experiment result is usually provided with spin parity J^P. Hence, in this work, the S-wave state means that a state can couple to two constituent particles, the $\Sigma^{(*)}_c \bar{D}^{(*)} - \Lambda_c \bar{D}^{(*)}$ here, in S wave while all other possible higher partial waves on L are included naturally.

Now we need treat an integral equation, to avoid divergence, a regularization is usually introduced. For example, a cutoff in momentum is introduced as one way to do the

regularization in the chiral unitary approach [41], which is related to the dimensional regularization [42]. In the qBSE approach, we usually adopt an exponential regularization by introducing a form factor into the propagator as

$$G_0(\mathrm{p}) \to G_0(\mathrm{p}) \left[e^{-(k_l^2 - m_l^2)^2/\Lambda_r^4} \right]^2, \tag{19}$$

where k_l and m_l are the momentum and mass of the lighter one of meson and baryon. The interested reader is referred to Ref. [37] for further information about the regularization. In Ref. [22], the authors warned that the π exchange provides excessive short-range interaction. In the current work, the relation of the cutoff $\Lambda_r = m + \alpha_r$ 0.22 GeV with m being the mass of the exchanged meson is also introduced into the regularization form factor as in those for the exchanged mesons. Such treatment will suppress the large-momentum, i.e., the short-range contribution of the π exchange.

The one-dimensional integral equation can be easily transformed into a matrix equation. The pole of scattering amplitude $\mathcal{M}$ can be searched by variation of z to satisfy $|1 - V(z)G(z)| = 0$ with $z = W + i\Gamma/2$ equaling to the system energy W at the real axis [37].

3 Single-channel results

The coupled-channel effect should be included into physical scattering. However, for the $\Sigma_c^{(*)}\bar{D}^{(*)} - \Lambda_c\bar{D}^{(*)}$ interaction considered in the current work, the coupled-channel effect should be small because the experimental pentaquarks are close to the thresholds. Our previous work [27] also supports such judgement. Moreover, the coupled-channel effect will make the results complex, which makes it difficult to show the property of bound states from each channels. Here, we will first present the results of a single-channel calculation.

3.1 Isodoublet bound states with $I = 1/2$

Now, we consider the isodoublet bound states from single-channel interaction. In the current work, we have two free parameters, cutoff parameters α_r and α_e for the regularization and the exchanged meson, respectively. In single-channel calculation here, we take $\alpha_r = \alpha_e = \alpha$ for simplification. Since the cutoff Λ should be about 1 GeV, we vary α in a range from 0.5 to 8.5 to find the bound state from each channel, which exhibits as a pole in the real axis of the complex plane of z. The obtained binding energies E_B with the variation of the α are illustrated in Fig. 1. Here, binding energy is defined as $E_B = M_{th} - W$ with M_{th} and W being the threshold and W of the pole.

In the current calculation, we consider ten interactions, $\Sigma_c\bar{D}$ with spin parity $1/2^-$, $\Sigma_c^*\bar{D}$ with $3/2^-$, $\Sigma_c\bar{D}^*$ with $1/2^-$ and $3/2^-$, $\Sigma_c^*\bar{D}^*$ with $1/2^-$, $3/2^-$, and $5/2^-$, $\Lambda_c\bar{D}^*$ with $1/2^-$ and $3/2^-$, and $\Lambda_c\bar{D}$ with $1/2^-$. With reasonable parameters, no bound state can be produced from the $\Lambda_c\bar{D}^*$ and $\Lambda_c\bar{D}$ interactions. For other seven interactions, the bound states are produced in the range of the α considered in the current calculation. Here, the results with different types of form factors for exchanged meson are presented in Fig. 1. The results show that the different choices of the form factors change the quantitive results but the qualitative conclusion are not changed. Moreover, the order of the curves for different form factors are almost the same for the seven bound states. It indicates that if appropriate cutoffs are adopted, the

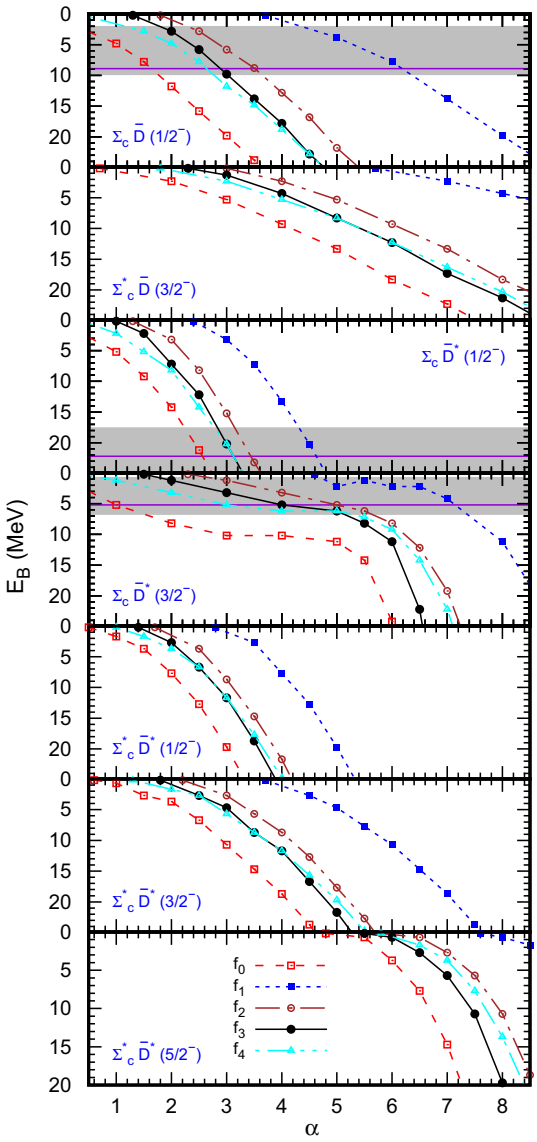

Fig. 1 The binding energy E_B with the variation of the α for isodoublet bound states from the single-channel interaction. The thresholds M_{th} for the $\Sigma_c\bar{D}$, $\Sigma_c^*\bar{D}$ and $\Sigma_c^*\bar{D}^*$ channels are 4320.8, 4385.3, 4462.2 and 4526.7 MeV, respectively. The f_i with $i = 0, 1, 2, 3, 4$ means the results without form factor for exchanged meson or with form factor $f_i(q^2)$ in Eqs. (11–14), respectively. The horizontal lines and the bands are the experimental mass and uncertainties observed at LHCb [1]

same conclusion can be reached with different choices of the form factors.

The $\Sigma_c\bar{D}$ bound state and two $\Sigma_c\bar{D}^*$ bound states can be related to the LHCb pentaquarks. Because there is only one S-wave bound state, the $P_c(4312)$ should be assigned into the $\Sigma_c\bar{D}(1/2^-)$ state in the molecular state picture. Two pentaquarks, $P_c(4457)$ and $P_c(4440)$ were observed at LHCb near the $\Sigma_c\bar{D}^*$ threshold, which can be related to two bound states with $1/2^-$ and $3/2^-$ from the $\Sigma_c\bar{D}^*$ interaction. For the $\Sigma_c\bar{D}^*(3/2^-)$ state, the binding energy increases to about 20 MeV at $\alpha = 2-3$ for form factor $f_{(0,2,3,4)}$ and α of about 5 for f_1. For the $\Sigma_c\bar{D}^*(1/2^-)$ state, in a large range of α, from 1 to about 6, the binding energy is smaller than 10 MeV. Such results suggest we should assign the $1/2^-$ state as $P_c(4440)$ and the $3/2^-$ state as $P_c(4457)$ state. Compared with experimental results, the α should be about 3 for $f_{(2,3,4)}$ and about 5 for f_1. With such choice, the $\Sigma_c\bar{D}(1/2^-)$ state has a binding energy about 10 MeV, which is quite consistent with the experimental value. The results also suggest that the form factor $f_{(2,3,4)}$ is more suitable to explain the three LHCb pentaquarks in the molecular state picture in the single-channel calculation.

Based on the above analysis, though the other four bound states, $\Sigma_c^*\bar{D}(3/2^-)$, $\Sigma_c^*\bar{D}^*(1/2^-)$, $\Sigma_c^*\bar{D}^*(3/2^-)$, $\Sigma_c^*\bar{D}^*(5/2^-)$, can be produced with variation of the cutoff, the existence of the $\Sigma_c^*\bar{D}^*(5/2^-)$ should be doubted because an α larger than 5 is required to produce such state, which is much larger the one to produce three LHCb pentaquarks with the experimental masses at the same time. If we adopt $\alpha = 3$ for the form factor $f_{(2,3,4)}$, the binding energies of $\Sigma_c^*\bar{D}^*(1/2^-)$ and $\Sigma_c^*\bar{D}^*(3/2^-)$ states are about 5 MeV, and the $\Sigma_c^*\bar{D}(3/2^-)$ state should have a very small binding energy.

3.2 Isoquartet bound states with $I = 3/2$

In the above, we present the isodoublet bound states. For the same interaction with different isospins, the model and parameters involved should be also the same. Hence, it is straight forward to give the prediction about the isoquartet bound states from the $\Sigma_c^{(*)}\bar{D}^{(*)}$ and $\Lambda_c\bar{D}^{(*)}$ interactions. The possible experimental observation about such bound states is also a good check to the molecular state interpretation of the LHCb pentaquarks and the results in this work. Here, we make the calculation to search isoquartet bound states in the same model as in the isodoulet case. The results are presented in Fig. 2.

Here, we still vary the α to search for the bound states from the interactions as in the isodoublet case. Generally speaking, a larger α should be adopted to produce the bound states. If we focus on the results with $f_{(2,3,4)}$, which is more suitable to reproduce the LHCb pentaquarks, the α is at least larger than 5 to produce a bound state from the interaction

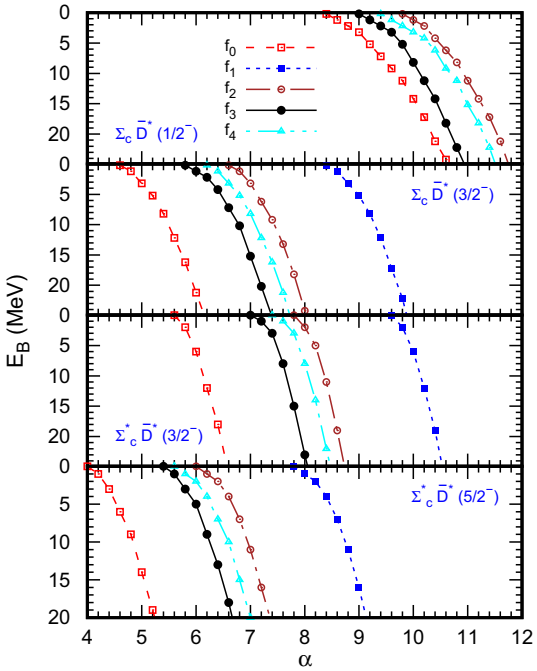

Fig. 2 The binding energy E_B with the variation of the α for isoquartet bound states. The other conventions are the same as in Fig. 1

considered here. With an α smaller than 12, no bound state can be found for the $\Sigma_c\bar{D}(1/2^-)$, the $\Sigma_c^*\bar{D}(3/2^-)$, and the $\Sigma_c^*\bar{D}^*(1/2^-)$ interactions. For the $\Sigma_c\bar{D}^*(1/2^-)$ interaction, an α larger than eight is required to force the potential strong enough to produce a bound state. For the $\Sigma_c\bar{D}^*(3/2^-)$ and $\Sigma_c^*\bar{D}^*(3/2^-)$ interactions, the bound states are produced at an α of about 6 GeV. The bound state from $\Sigma^*\bar{D}^*(5/2^-)$ appears at an α of about five for $f_{(2,3,4)}$ and more larger for f_1. If we recall that the LHCb pentaquarks are reproduced at an α of three for $f_{(2,3,4)}$ and five for f_1 in the isodoublet case, it is reasonable to doubt the existence of the four bound states shown in Fig. 2 if the assignment of three LHCb pentaquarks are right.

Usually, increase of the α can enhance the strength of the interaction. The large α required here suggest that the isoquaret interactions are much weaker than those with $I = 1/2$. It is easy to understand if we recall the flavor factors listed in Table 2. The sign between the potentials by π and η exchanges, and that between ρ and ω exchanges is different for $I = 1/2$ and $3/2$ cases. It results in the cancellation of two contributions in the isoquaret case. Such cancellation makes the interaction with $I = 3/2$ too weak to produce a bound state with a small α.

4 Coupled-channel results

It is well known that the coupled-channel effect will affect the binding energy of the bound state. Moreover, if a lower

channel was considered, the bound state from the channel with higher threshold will acquire a width. In the above single-channel calculation, six bound states are produced [the $\Sigma_c^*\bar{D}(5/2^-)$ is not well supported because a large α is required]. Those states are from three channels, which can be coupled to each other by light meson exchange as the single-channel interaction. With the Lagrangians in the heavy quark limit and chiral symmetry, a coupled-channel calculation can be preformed for the $\Sigma_c^{(*)}\bar{D}^{(*)} - \Lambda_c\bar{D}^{(*)}$ interaction.

4.1 The poles from the $\Sigma_c^{(*)}\bar{D}^{(*)} - \Lambda_c\bar{D}^{(*)}$ interaction

In single-channel calculation, the bound state is a pole at real axis. After the coupled-channel effect are included, the pole will leave the real axis and becomes a pole in the complex plane as shown in Fig. 3. The poles from the $\Sigma_c^{(*)}\bar{D}^{(*)} - \Lambda_c\bar{D}^{(*)}$ interaction with $J^P = 1/2^-$ and $3/2^-$ are presented in the figure.

Here we take the f_3 to show the coupled channel results. The results with $f_{(1,2,4)}$ is qualitatively consistent with the results with f_3 if the cutoff is varies correspondingly. In the single-channel calculation, the best value of α is found about three to reproduce the experimental masses of three LHCb pentaquarks. After including the coupled-channel effect, besides the bound states have width and become resonances, the masses of the resonances are also different from the masses obtained from the single-channel calculation. If we still adopt an α of three, the pole of the $\Sigma_c\bar{D}(1/2^-)$ state will move from 4311 to 4294 MeV, which is even below the $\Lambda_c\bar{D}^*$ threshold. Hence, we adopt a smaller value α of 2.5 to give the poles from the $\Sigma_c^{(*)}\bar{D}^{(*)} - \Lambda_c\bar{D}^{(*)}$ interaction.

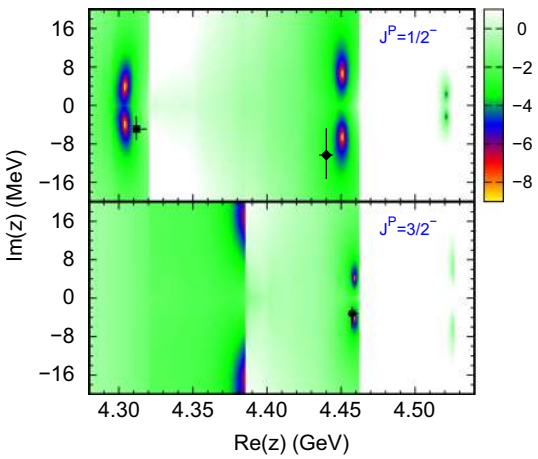

Fig. 3 The $\log|1-V(z)G(z)|$ with the variation of z for the $\Sigma_c^{(*)}\bar{D}^{(*)}-\Lambda_c\bar{D}^{(*)}$ interaction with $J^P = 1/2^-$ and $3/2^-$ at $\alpha = 2.5$. The color means the value of $\log|1 - V(z)G(z)|$ as shown in the color box. The form factor f_3 is adopted in the calculation. The full square, diamond, and circle are for the experimental data of the $P_c(4312)$, $P_c(4440)$ and $P_c(4457)$ at LHCb [1]

Six poles can be found in the complex plane with their conjugate partners. In the case with $J^P = 1/2^-$, there exist three poles near the $\Sigma_c\bar{D}$, $\Sigma_c\bar{D}^*$ and $\Sigma^*\bar{D}^*$ thresholds, respectively. In the case with $J^P = 3/2^-$, we also have three poles near the $\Sigma_c^*\bar{D}$, $\Sigma_c\bar{D}^*$ and $\Sigma^*\bar{D}^*$ thresholds, respectively. The pole near the $\Sigma_c\bar{D}$ threshold is obviously related to the $P_c(4312)$. Compared with experimental values at LHCb, $M = 4311.9\pm0.7^{+6.8}_{-0.6}$ and $\Gamma = 9.8\pm2.7^{+3.7}_{-4.5}$ MeV, the theoretical pole at $4304-4i$ MeV is a little lower but in the uncertainties of the width [here we use the relation $\Gamma = -2\,\mathrm{Im}(z)$]. Two poles appear near the $\Sigma_c\bar{D}^*$ with $1/2^-$ and $3/2^-$, respectively. The pole in $3/2^-$ fall in the experimental values with uncertainties quite well while the $1/2^-$ pole is a little higher in mass. Though the mass gap of these two states is narrowed after the coupled-channel effect included, the order of these two states still supports the assignment of two states with $1/2^-$ and $3/2^-$ as $P_c(4440)$ and $P_c(4457)$, respectively. The theoretical widths also support such assignment. Hence, as the single-channel results, the coupled-channel results support the assignment of the $P_c(4457)$, $P_c(4440)$ and $P_c(4312)$ as molecular states $\Sigma_c\bar{D}(1/2^-)$, $\Sigma_c\bar{D}^*(1/2^-)$ and $\Sigma_c\bar{D}(3/2^-)$, respectively.

It is interesting to observe a pole near the $\Sigma^*\bar{D}$ threshold, which may be related to the $P_c(4380)$ suggested in the old LHCb article [2]. This pole is almost on the threshold, if the physical strength of the interaction is a little weaker, it may become a cusp on the threshold. Besides, it has a width about 40 MeV, which is much larger than three LHCb pentaquarks. These properties of this state may be the reason why the $P_c(4380)$ is very broad and difficult to be observed in the invariant mass spectrum.

Near the $\Sigma^*\bar{D}^*$ threshold, two poles can be found with both $1/2^-$ and $3/2^-$. The $1/2^-$ pole is at $4521-2i$ and $3/2^-$ pole is at $4526-2i$. These two poles are obviously shallower than other poles. It indicates that the peaks corresponding of these states may be smaller than other states.

4.2 The widths of the molecular states

From the above results, we can find that the widths of the P_c states can be well reproduced in our model. It is interesting to give the widths from each channel to show the strength of the coupling between the molecular state and the corresponding channel. In the current work, the pole of a molecular in the complex plane can be obtained by a coupled-channel calculation. Usually, the width of a state can be obtained as $\Gamma = -2\mathrm{Im}(z)$ where the z is the position of the pole, that is, the width can be related to the imaginary part of the pole. In Table 3, we list the poles of the molecular states for full coupled-channel calculation and two-channel calculation.

From the analysis in Secti. 4.1, one can find that the coupled-channel effects between different channels will effect the position of the poles but not very far. We can still

Table 3 The positions and branching ratios of the molecular states. The "CC" means the full coupled-channel calculaiton. The "pole" means mass of corresponding threshold subtracted by the position of a pole, $M_{th} - z$, in the unit of MeV and Br= $\frac{\text{Im}_i}{\sum \text{Im}_i}$ for i channel in the unit of %. The α_r is the cutoff in the exponential regularization in Eq. (19). The explicit explanation can be found in the text

α_r	CC	$\Sigma_c\bar{D}^*$		$\Sigma^*_c\bar{D}$		$\Sigma_c\bar{D}$		$\Lambda_c\bar{D}^*$		$\Lambda_c\bar{D}$		Sum	
	pole	pole	Br	pole	Br	pole	Br	pole	Br	pole	Br	$\sum \text{Im}_i$	$\frac{\text{Im}_{CC}}{\sum \text{Im}_i}$
$\Sigma^*_c\bar{D}^*(1/2^-)$													
1.5	$1.2+1.0i$	$1.8+0.1i$	17	$2.1+0.1i$	17	$1.2+0.3i$	50	$1.7+0.1i$	17	$1.9+0.0i$	0	0.6	167
2.0	$3.0+1.6i$	$3.7+0.2i$	18	$3.9+0.2i$	18	$2.9+0.5i$	45	$4.6+0.2i$	18	$3.7+0.0i$	0	1.1	145
2.5	$5.5+2.3i$	$6.1+0.3i$	19	$6.6+0.3i$	19	$5.3+0.7i$	44	$6.4+0.3i$	19	$6.4+0.0i$	0	1.6	144
3.0	$7.4+3.1i$	$8.8+0.4i$	18	$9.0+0.4i$	18	$7.1+1.0i$	45	$8.4+0.4i$	10	$9.2+0.0i$	0	2.2	141
$\Sigma^*_c\bar{D}^*(3/2^-)$													
2.0	$0.0+4.2i$	$0.3+0.7i$	28	$0.5+0.7i$	28	$1.2+0.0i$	0	$0.0+0.9i$	36	$1.1+0.2i$	8	2.5	168
2.5	$0.0+5.8i$	$1.0+1.2i$	32	$1.1+0.8i$	22	$2.3+0.0i$	0	$0.0+1.5i$	41	$2.3+0.2i$	5	3.7	158
3.0	$0.0+6.8i$	$1.7+1.7i$	37	$1.6+1.0i$	22	$3.4+0.0i$	0	$0.0+1.7i$	37	$3.4+0.2i$	4	4.6	148
3.5	$0.0+7.5i$	$2.2+2.1i$	41	$2.0+1.1i$	22	$4.2+0.1i$	2	$0.0+1.5i$	29	$4.4+0.3i$	6	5.1	147
$\Sigma_c\bar{D}^*(1/2^-)$													
1.0	$3.5+1.9i$	–	–	$3.0+0.0i$	0	$2.9+0.3i$	20	$3.3+1.2i$	80	$3.0+0.0i$	0	1.5	127
2.0	$8.2+4.8i$	–	–	$8.7+0.2i$	5	$8.0+0.5i$	12	$9.1+3.3i$	80	$8.7+0.1i$	2	4.1	117
3.0	$13.8+8.8i$	–	–	$15.2+0.9i$	11	$14.1+0.8i$	9	$15.5+6.3i$	74	$16.2+0.5i$	6	8.5	104
4.0	$17.7+14.7i$	–	–	$23.2+2.1i$	15	$19.0+1.5i$	11	$21.5+9.4i$	66	$22.1+1.2i$	9	14.2	104
$\Sigma_c\bar{D}^*(3/2^-)$													
1.0	$2.7+1.0i$	–	–	$1.8+0.3i$	19	$1.6+0.0i$	0	$1.4+1.0i$	63	$1.6+0.3i$	19	1.6	63
1.5	$3.5+2.3i$	–	–	$2.1+0.4i$	13	$2.0+0.0i$	0	$0.9+2.4i$	75	$1.7+0.4i$	13	3.2	72
2.0	$3.4+3.6i$	–	–	$2.1+0.4i$	9	$2.1+0.1i$	2	$0.0+3.5i$	78	$1.6+0.5i$	11	4.5	80
2.5	$2.8+4.2i$	–	–	$2.1+0.4i$	12	$2.0+0.1i$	3	$0.0+2.4i$	71	$1.4+0.5i$	15	3.4	81
3.0	$2.6+4.5i$	–	–	$2.0+0.4i$	13	$2.0+0.1i$	3	$0.0+2.0i$	65	$1.4+0.6i$	19	3.1	69
$\Sigma_c^*\bar{D}(3/2^-)$													
2.5	$0.0+19i$	–	–	–	–	$0.4+0i$	0	$0.0+16i$	100	$0.4+0i$	0	16	119
3.0	$0.0+24i$	–	–	–	–	$0.6+0i$	0	$0.0+19i$	100	$0.6+0i$	0	19	126
3.5	$0.0+28i$	–	–	–	–	$0.9+0i$	0	$0.0+22i$	100	$0.9+0i$	0	22	127
4.0	$0.0+30i$	–	–	–	–	$1.0+0i$	0	$0.0+25i$	100	$1.0+0i$	0	25	120
$\Sigma_c\bar{D}(1/2^-)$													
1.0	$3.7+2.0i$	–	–	–	–	–	–	$3.4+2.1i$	88	$2.1+0.3i$	13	2.4	83
1.5	$8.1+2.9i$	–	–	–	–	–	–	$6.1+3.0i$	88	$3.3+0.4i$	12	3.4	85
2.0	$11.4+4.0i$	–	–	–	–	–	–	$9.4+4.0i$	89	$4.6+0.5i$	11	4.5	89
2.5	$17.8+4.6i$	–	–	–	–	–	–	$13.6+4.9i$	87	$5.9+0.7i$	13	5.6	82
3.0	$23.6+4.8i$	–	–	–	–	–	–	$18.4+5.1i$	86	$7.1+0.8i$	14	5.9	81

identify the main contribution of a molecular state from its mass. Here, we remark the states with their main origin, for example, for the state near $\Sigma_c^*\bar{D}^*$ thresholds with $1/2^-$, we adopt a notation as $\Sigma_c^*\bar{D}^*(1/2^-)$. In Table 3, the results for six states $\Sigma_c^*\bar{D}^*(1/2^-)$ $\Sigma_c^*\bar{D}^*(3/2^-)$, $\Sigma_c\bar{D}^*(1/2^-)$, $\Sigma_c\bar{D}^*(3/2^-)$, $\Sigma_c^*\bar{D}(3/2^-)$ and $\Sigma_c\bar{D}(1/2^-)$, which can be produced with an α in a reasonable region where the LHCb pentaquarks can be reproduced, are presented in order. The positions of the these states with the full coupled-channel calculation are listed in second column in Table 3. Here, to emphasize the binding energy, we replace the real part of the pole by the binding energy, that is, $z \to M_{th} - z$ with M_{th} being the mass of the threshold.

In third to twelfth columns, we present the results from the two-channel calculation. In such calculation, we only keep the coupling between main channel and another channel to study the effect of this channel on the bound state from the main channel. Again, we take the $\Sigma_c^*\bar{D}^*(1/2^-)$ given first in Table 3 as example. For this case, the $\Sigma_c^*\bar{D}^*$ is the main channel. The $\Sigma_c^*\bar{D}^*(1/2^-)$ state is mainly produced from this interaction. If only $\Sigma_c^*\bar{D}^*$ channel is considered, the pole is at the real axis. After another channel, such as $\Sigma_c\bar{D}^*$, is

added, the pole will move to complex plane. Especially, the imaginary part or width of this state is from the $\Sigma_c\bar{D}^*$ channel totally in such two-channel calculation. In Table 3, the results for two-channel calculation from main channel and one of the $\Sigma_c\bar{D}^*$, $\Sigma_c^*\bar{D}$, $\Sigma_c\bar{D}$, $\Lambda_c\bar{D}^*$, and $\Lambda_c\bar{D}$ channels are given from third to twelfth columns in order. Here, we introduce the branching ratio Br to present the importance of corresponding channel. It is defined as the imaginary part of the each channel divided by the sum of the imaginary parts of all channels, that is, $\mathrm{Br} = \frac{\mathrm{Im}_i}{\sum \mathrm{Im}_i}$. The results with different values of α_r are presented to show the stability of the branching ratios. One can find that the sum of the imaginary parts of every channels, listed in the thirteenth column, deviates from the full coupled-channel result, which is shown in the last column as $\frac{\mathrm{Im}_{CC}}{\sum \mathrm{Im}_i}$. It is from the couplings between the channels except the main channel $\Sigma_c^*\bar{D}^*$. Such deviation is small in all cases. Hence, the branching ratio here should be seen as the first order approximation if the pole of the molecular state is not far away from the threshold of the its main origin.

Two $\Sigma_c^*\bar{D}^*$ states can decay into five channels considered in this work. In the full coupled-channel calculation, the real and imaginary parts of the pole increase with the increase of α_r. Such behavior can be also found in the two-channel results. However, the branching ratio of each channel is not sensitive to the variation of the parameter. The $\Sigma_c\bar{D}$ is the most important decay channel of the $\Sigma_c^*\bar{D}^*(1/2^-)$ state with a branching about 50%, and the $\Sigma_c\bar{D}^*$, $\Sigma_c^*\bar{D}$ and $\Lambda_c\bar{D}^*$ channels also have considerable contributions with branching ratios a little smaller than 20%. The $\Lambda_c\bar{D}$ channel has little effect on the decay width of the $\Sigma_c^*\bar{D}^*(1/2^-)$ state (here and hereafter the $0.0i$ does not means forbidding but a very small width in the current precision). For the $\Sigma_c^*\bar{D}^*(3/2^-)$ state, the $\Sigma_c\bar{D}^*$, $\Sigma_c^*\bar{D}$ and $\Lambda_c\bar{D}^*$ channels provide considerable widths with branching ratios about 20–30%, while its couplings to the $\Sigma_c\bar{D}$ and $\Lambda_c\bar{D}$ channels are very small.

There exist two states near the $\Sigma_c\bar{D}^*$ threshold in our model, which can be related to the experimental $P_c(4440)$ and $P_c(4457)$. The channel above the $\Sigma_c\bar{D}^*$ channel, here $\Sigma_c^*\bar{D}^*$ channel, does not provide the width, that is, the the pole near the $\Sigma_c\bar{D}^*$ threshold from the two-channel calculation with $\Sigma^*\bar{D}^*$ channel is still on the real axis. It reflects that a state $\Sigma\bar{D}^*$ can not decay to $\Sigma^*\bar{D}^*$ which is beyond its mass. Hence, there are only four channels listed. For both $\Sigma_c\bar{D}^*$ states, the $\Lambda\bar{D}^*$ channel is dominant, with branching ratio about 70%. Other channels only have branching ratios smaller than 20%. The dominance of the $\Lambda_c\bar{D}^*$ is also found in the $\Sigma_c^*\bar{D}(3/2^-)$ and $\Sigma_c\bar{D}(1/2^-)$ states, where fewer channels are opened in the models considered in the current work. The branching ratio of the $\Sigma_c^*\bar{D}(3/2^-)$ state to the $\Lambda_c\bar{D}$ channel is 100% while the $\Lambda_c\bar{D}$ channel provides about 90% contribution to the $\Sigma_c\bar{D}(1/2^-)$ state.

5 Summary and discussion

In this work, the $\Sigma_c^{(*)}\bar{D}^{(*)} - \Lambda_c\bar{D}^{(*)}$ interaction is studied in the qBSE approach with the help of the Lagrangians in heavy quark limit and with chiral symmetry. The single-channel calculation shows that three LHCb pentaquarks, $P_c(4312)$, $P_c(4440)$, and $P_c(4457)$ can be well reproduced from the $\Sigma_c\bar{D}$ interaction with spin parity $J^P = 1/2^-$ and $\Sigma_c\bar{D}^*$ interaction with $1/2^-$ and $3/2^-$, respectively. It is further supported by the coupled-channel calculation, where the bound states become poles in the complex plane, and acquire widths in the uncertainties of the experimental values. Our results also suggest that the $P_c(4440)$ and $P_c(4457)$ should have large branching ratios in the $\Lambda_c\bar{D}^*$ channel, and this channel is also very important in the decay of the $P_c(4312)$. The $P_c(4380)$, which is suggested by the first LHCb experiment and suspended in the updated results, can be related to the $\Sigma_c^*\bar{D}$ state with $3/2^-$. This state is on the $\Sigma_c^*\bar{D}$ threshold and has a large width from $\Lambda\bar{D}^*$ channel. It may be only a cusp on the threshold. If so, the peak in the invariant mass spectrum of this state will be broad and difficult to be distinguished in experiment.

Other possible molecular states from the $\Sigma_c^{(*)}\bar{D}^{(*)} - \Lambda_c\bar{D}^{(*)}$ interaction are also predicted in the same model. three $\Sigma_c^*\bar{D}^*$ states can be produced with appropriate α adopted. However, very large α are required to produce the state with $5/2^-$. Such results are consistent with the Scenario A of Ref. [23], where the binding energy of the state with $5/2^-$ is the smallest. If we adopt a value of α which can reproduce three LHCb pentaquark, only two states, $\Sigma_c^*\bar{D}^*$ with $1/2^-$ and $3/2^-$ are suggested by our results. The decay patterns of this two states are also studied in the coupled-channel calculation. The $\Sigma_c\bar{D}$ channel is found important to the state with $1/2^-$ and three channels, $\Sigma_c\bar{D}^*$, $\Sigma^*\bar{D}$, and $\Lambda_c\bar{D}$ have considerable contributions to the state with $3/2^-$. The isoquaret molecular states with $I = 3/2$ are also studied in the same model. The results suggest that the interaction is very weak. Only three states, $\Sigma_c\bar{D}(1/2^-)$, $\Sigma^*\bar{D}^*(3/2^-)$, and $\Sigma_c\bar{D}(5/2^-)$ can be produced but very large α are required.

Acknowledgements This project is supported by the National Natural Science Foundation of China (Grants No. 11675228, and No. 11375240), and the Fundamental Research Funds for the Central Universities.

Data Availability Statement This manuscript has no associated data or the data will not be deposited. [Authors' comment: The current work is a theoretical work. All results have been presented in Figs. 1, 2, 3 and Table 1.]

Funded by SCOAP[3].

References

1. R. Aaij et al. [LHCb Collaboration], Phys. Rev. Lett. **122** (2019) 22, 222001 arXiv:1904.03947 [hep-ex]
2. R. Aaij et al., [LHCb Collaboration] "Observation of $J/\psi p$ resonances consistent with pentaquark states in $\Lambda_b^0 \to J/\psi K^- p$ decays". Phys. Rev. Lett. **115**, 072001 (2015). arXiv:1507.03414 [hep-ex]
3. J.J. Wu, R. Molina, E. Oset, B.S. Zou, Prediction of narrow N^* and Λ^* resonances with hidden charm above 4 GeV. Phys. Rev. Lett. **105**, 232001 (2010)
4. W.L. Wang, F. Huang, Z.Y. Zhang, B.S. Zou, $\Sigma_c \bar{D}$ and $\Lambda_c \bar{D}$ states in a chiral quark model. Phys. Rev. C **84**, 015203 (2011). arXiv:1101.0453 [nucl-th]
5. Z.C. Yang, Z.F. Sun, J. He, X. Liu, S.L. Zhu, The possible hidden-charm molecular baryons composed of anti-charmed meson and charmed baryon. Chin. Phys. C **36**, 6 (2012). arXiv:1105.2901 [hep-ph]
6. J.J. Wu, T.-S.H. Lee, B.S. Zou, Nucleon resonances with hidden charm in coupled-channel models. Phys. Rev. C **85**, 044002 (2012). arXiv:1202.1036 [nucl-th]
7. R. Chen, X. Liu, X.Q. Li, S.L. Zhu, Identifying exotic hidden-charm pentaquarks. Phys. Rev. Lett. **115**(13), 132002 (2015). arXiv:1507.03704 [hep-ph]
8. H.X. Chen, W. Chen, X. Liu, T.G. Steele, S.L. Zhu, Towards exotic hidden-charm pentaquarks in QCD. Phys. Rev. Lett. **11517**, 172001 (2015). arXiv:1507.03717 [hep-ph]
9. M. Karliner, J.L. Rosner, Phys. Rev. Lett. **115**(12), 122001 (2015). arXiv:1506.06386 [hep-ph]
10. L. Roca, J. Nieves, E. Oset, LHCb pentaquark as a $\bar{D}^* \Sigma_c - \bar{D}^* \Sigma_c^*$ molecular state. Phys. Rev. D **929**, 094003 (2015). arXiv:1507.04249 [hep-ph]
11. J. He, $\bar{D} \Sigma_c^*$ and $\bar{D}^* \Sigma_c$ interactions and the LHCb hidden-charmed pentaquarks. Phys. Lett. B **753**, 547 (2016). arXiv:1507.05200 [hep-ph]
12. T.J. Burns, Phenomenology of $P_c(4380)^+$, $P_c(4450)^+$ and related states. Eur. Phys. J. A **5111**, 152 (2015). arXiv:1509.02460 [hep-ph]
13. J. He, Understanding spin parity of $P_c(4450)$ and $Y(4274)$ in a hadronic molecular state picture. Phys. Rev. D **957**, 074004 (2017). arXiv:1607.03223 [hep-ph]
14. R. Chen, X. Liu, Z. F. Sun, S. L. Zhu, "Strong LHCb evidence for supporting the existence of hidden-charm molecular pentaquarks," arXiv:1903.11013 [hep-ph]
15. H. X. Chen, W. Chen, S. L. Zhu, "Possible interpretations of the $P_c(4312)$, $P_c(4440)$, and $P_c(4457)$," arXiv:1903.11001 [hep-ph]
16. C. Fernández-Ramírez *et al.* [JPAC Collaboration], "Interpretation of the LHCb Pc(4312) Signal," Phys. Rev. Lett. **123** (2019) 9, 092001. arXiv:1904.10021 [hep-ph]
17. Q. Wu, D. Y. Chen, "Production of P_c states from Λ_b decay," arXiv:1906.02480 [hep-ph]
18. Z. G. Wang, "Analysis of the $\bar{D} \Sigma_c$, $\bar{D} \Sigma_c^*$, $\bar{D}^* \Sigma_c$ and $\bar{D}^* \Sigma_c^*$ pentaquark molecular states with QCD sum rules," Int. J. Mod. Phys. A **34** (2019) no.19, 1950097. arXiv:1806.10384 [hep-ph]
19. H. Huang, J. He, J. Ping, "Looking for the hidden-charm pentaquark resonances in $J/\psi p$ scattering," arXiv:1904.00221 [hep-ph]
20. H. Huang, C. Deng, J. Ping, F. Wang, Possible pentaquarks with heavy quarks. Eur. Phys. J. C **76**(11), 624 (2016)
21. M. Z. Liu, Y. W. Pan, F. Z. Peng, M. Sánchez Sánchez, L. S. Geng, A. Hosaka, M. Pavon Valderrama, "Emergence of a complete heavy-quark spin symmetry multiplet: seven molecular pentaquarks in light of the latest LHCb analysis," Phys. Rev. Lett. **122** no.24, 242001 (2019). arXiv:1903.11560 [hep-ph]
22. M. Z. Liu, T. W. Wu, M. Sánchez Sánchez, M. P. Valderrama, L. S. Geng, J. J. Xie, "Spin-parities of the $P_c(4440)$ and $P_c(4457)$ in the one-Boson-exchange model," arXiv:1907.06093 [hep-ph]
23. Y. W. Pan, M. Z. Liu, F. Z. Peng, M. Sánchez Sánchez, L. S. Geng, M. Pavon Valderrama, "Model independent determination of the spins of the $P_c(4440)$ and $P_c(4457)$ from the spectroscopy of the triply charmed dibaryons," arXiv:1907.11220 [hep-ph]
24. Y.H. Lin, C.W. Shen, B.S. Zou, Decay behavior of the strange and beauty partners of P_c hadronic molecules. Nucl. Phys. A **980**, 21 (2018). arXiv:1805.06843 [hep-ph]
25. Y. H. Lin, B. S. Zou, "Strong decays of the latest LHCb pentaquark candidates in hadronic molecule pictures," arXiv:1908.05309 [hep-ph]
26. C.J. Xiao, Y. Huang, Y.B. Dong, L.S. Geng, D.Y. Chen, Exploring the molecular scenario of Pc(4312), Pc(4440), and Pc(4457). Phys. Rev. D **1001**, 014022 (2019). arXiv:1904.00872 [hep-ph]
27. J. He, Study of $P_c(4457)$, $P_c(4440)$, and $P_c(4312)$ in a quasipotential Bethe–Salpeter equation approach. Eur. Phys. J. C **79**(5), 393 (2019). arXiv:1903.11872 [hep-ph]
28. H.Y. Cheng, C.Y. Cheung, G.L. Lin, Y.C. Lin, T.M. Yan, H.L. Yu, Chiral Lagrangians for radiative decays of heavy hadrons. Phys. Rev. D **47**, 1030 (1993). arXiv:hep-ph/9209262
29. T. M. Yan, H. Y. Cheng, C. Y. Cheung, G. L. Lin, Y. C. Lin, H. L. Yu, "Heavy quark symmetry and chiral dynamics," Phys. Rev. D **46**, 1148 (1992) Erratum: [Phys. Rev. D **55**, 5851 (1997)]
30. M.B. Wise, Chiral perturbation theory for hadrons containing a heavy quark. Phys. Rev. D **45**, 2188 (1992)
31. R. Casalbuoni, A. Deandrea, N. Di Bartolomeo, R. Gatto, F. Feruglio, G. Nardulli, Phenomenology of heavy meson chiral Lagrangians. Phys. Rept. **281**, 145 (1997). arXiv: hep-ph/9605342
32. M. Tanabashi et al., [Particle Data Group]. Phys. Rev. D **983**, 030001 (2018). https://doi.org/10.1103/PhysRevD.98.030001
33. Y.R. Liu, M. Oka, $\Lambda_c N$ bound states revisited. Phys. Rev. D **85**, 014015 (2012). arXiv:1103.4624 [hep-ph]
34. C. Isola, M. Ladisa, G. Nardulli, P. Santorelli, Charming penguins in $B \to K^* \pi$, $K(\rho, \omega, \phi)$ decays. Phys. Rev. D **68**, 114001 (2003). arXiv:hep-ph/0307367
35. A.F. Falk, M.E. Luke, Strong decays of excited heavy mesons in chiral perturbation theory. Phys. Lett. B **292**, 119 (1992). arXiv:hep-ph/9206241
36. J. He, Study of the $B\bar{B}^*/D\bar{D}^*$ bound states in a Bethe–Salpeter approach. Phys. Rev. D **907**, 076008 (2014). arXiv:1409.8506 [hep-ph]
37. J. He, The $Z_c(3900)$ as a resonance from the $D\bar{D}^*$ interaction. Phys. Rev. D **923**, 034004 (2015). arXiv:1505.05379 [hep-ph]
38. J. He, D.Y. Chen, X. Liu, New Structure Around 3250 MeV in the Baryonic B Decay and the $D_0^*(2400)N$ Molecular Hadron. Eur. Phys. J. C **72**, 2121 (2012). arXiv:1204.6390 [hep-ph]
39. J. He, Internal structures of the nucleon resonances N (1875) and N(2120). Phys. Rev. C **911**, 018201 (2015). arXiv:1501.00522 [nucl-th]
40. J. He, Nucleon resonances $N(1875)$ and $N(2100)$ as strange partners of LHCb pentaquarks. Phys. Rev. D **957**, 074031 (2017). arXiv:1701.03738 [hep-ph]
41. E. Oset, A. Ramos, Nonperturbative chiral approach to s wave anti-K N interactions. Nucl. Phys. A **635**, 99 (1998). arXiv:nucl-th/9711022
42. J. A. Oller, E. Oset, J. R. Pelaez, "Meson meson interaction in a nonperturbative chiral approach," Phys. Rev. D **59**, 074001 (1999) Erratum: [Phys. Rev. D **60**, 099906 (1999)] Erratum: [Phys. Rev. D **75**, 099903 (2007)]